

Impact of Reactive Amphiphilic Copolymers on Mechanical Properties and Cell Responses of Fibrin-Based Hydrogels

Miriam Aischa Al Enezy-Ulbrich, Hanna Malyaran, Robert Dirk de Lange, Norina Labude, René Plum, Stephan Rütten, Nicole Terefenko, Svenja Wein, Sabine Neuss, and Andrij Pich*

Mechanical properties of hydrogels can be modified by the variation of structure and concentration of reactive building blocks. One promising biological source for the synthesis of biocompatible hydrogels is fibrinogen. Fibrinogen is a glycoprotein in blood, which can be transformed enzymatically to fibrin playing an important role in wound healing and clot formation. In the present work, it is demonstrated that hybrid hydrogels with their improved mechanical properties, tunable internal structure, and enhanced resistance to degradation can be synthesized by a combination of fibrinogen and reactive amphiphilic copolymers. Water-soluble amphiphilic copolymers with tunable molecular weight and controlled amounts of reactive epoxy side groups are used as reactive crosslinkers to reinforce fibrin hydrogels. In the present work, copolymers that can influence the mechanical properties of fibrin-based hydrogels are used. The reactive copolymers increase the storage modulus of the hydrogels from 600 Pa to 30 kPa. The thickness of fibrin fibers is regulated by the copolymer concentration. It could be demonstrated that the fibrin-based hydrogels are biocompatible and support cell proliferation. Their degradation rate is considerably slower than that of native fibrin gels. In conclusion, fibrin-based hydrogels with tunable elasticity and fiber thickness useful to direct cell responses like proliferation and differentiation are produced.

2.5 g L⁻¹ and is essential for haemostasis, wound healing, inflammation, angiogenesis, and other biological functions.^[1–4] Fibrin is a large biopolymer synthesized from its precursor fibrinogen, which is assembled to fibrin triggered by thrombin. Thrombin induces the oligomer and protofibril formation of fibrinogen. These oligomers and protofibrils self-assemble to bigger protofibrils and become fibrin fibers.^[3] Through fibrinolysis, the formed blood clot of fibrin can be dissolved, resulting in fibrin degradation products called fibrinopeptides and D-Dimers. The clot is cleaved by plasmin, a proteolytic enzyme, which is activated from plasminogen on the fibrin surface.^[5] Fibrin can also be used as a biopolymer with excellent characteristics for tissue engineering applications and regenerative medicine, for example, as extracellular matrix (ECM) component in 3D constructs. Since fibrin is the main component in clot formation, it shows interesting mechanical properties.^[3] Biological tissues show nonlinear elastic


1. Introduction

Fibrinogen, also known as factor I in the blood clotting cascade, is a fibrous glycoprotein, with a mass of 340 kDa (kilodalton), present in human blood plasma at a concentration of about

behavior to prevent large deformation. That means they are getting stiffer with an increasing strain. This strain-stiffening is typical for any networks consisting of semiflexible and filamentous proteins because of their hierarchical structure. No high geometrical arrangement is needed to obtain this behavior because it is

M. A. Al Enezy-Ulbrich, R. D. de Lange, R. Plum, N. Terefenko, Prof. A. Pich
Functional and Interactive Polymers
Institute of Technical and Macromolecular Chemistry
RWTH Aachen University
Worringerweg 1, Aachen 52074, Germany
E-mail: pich@dwi.rwth-aachen.de

M. A. Al Enezy-Ulbrich, R. D. de Lange, R. Plum, N. Terefenko, Prof. A. Pich
DWI – Leibniz Institute for Interactive Materials
RWTH Aachen University
Forckenbeckstraße 50, Aachen 52074, Germany

 The ORCID identification number(s) for the author(s) of this article can be found under <https://doi.org/10.1002/adfm.202003528>.

© 2020 The Authors. Published by WILEY-VCH Verlag GmbH & Co. KGaA, Weinheim. This is an open access article under the terms of the Creative Commons Attribution License, which permits use, distribution and reproduction in any medium, provided the original work is properly cited.

H. Malyaran, N. Labude, S. Wein, Prof. S. Neuss
Helmholtz Institute for Biomedical Engineering
BioInterface Group
RWTH Aachen University
Pauwelsstrasse 20, Aachen 52074, Germany

H. Malyaran, N. Labude, S. Wein, Prof. S. Neuss
Institute of Pathology
RWTH Aachen University
Pauwelsstrasse 30, Aachen 52074, Germany
S. Rütten
Electron Microscopic Facility
University Clinics
RWTH Aachen University
Pauwelsstrasse 30, Aachen 52074, Germany

DOI: 10.1002/adfm.202003528

fundamental for isotropic networks based on semiflexible polymers, which are crosslinked.^[6] Strain-stiffening has also a high impact on cells in cell cultures. Cells show different behavior due to their environmental conditions. The spatial environment is of main importance for cell characteristics and function. It is well-known, that cells grow differentially depending on whether they are in a 3D matrix or on a 2D surface. This was already demonstrated by Petersen et al. in 1992 with breast epithelial cells, which proliferated like tumor cells on a 2D layer. Compared to a 3D matrix, they express many genes which are characteristic for tumor cells.^[7] Studies demonstrate that embryonic stem cells can differentiate in a 3D scaffold more efficiently than on a 2D substrate.^[8] Cells in gels with a linear elastic behavior are roundish and do not exhibit shape deformation on soft gels. Contrary, the cells are more spread with an increasing modulus of the substrate they are growing on. Cells on nonlinear elastic gels spread maximally and are also influenced by cells localized at a certain distance.^[9] The excellent biocompatibility and 3D processable capabilities of fibrin hydrogels have made them suitable candidates for various bioartificial manufacturing processes in tissue engineering. The polymerized fibrin gel matrix is a hydrogel, which contains ≈95–98% water. The water content can easily be exchanged against a buffer solution or a cell culture medium, allowing for an optimal nutrition supply of the cells that are embedded in the hydrogel.^[10] Over the past decades, many fundamental and preclinical studies have been conducted to investigate the therapeutic utility of mesenchymal stem cells (MSCs) in the treatment of diseases and injuries, such as neurodegenerative diseases,^[11] spinal cord injury,^[12] and cardiovascular diseases.^[13] In most of these studies, treatment with MSCs resulted in significant functional benefits because of their trophic characteristics. The stem cells injected into injured or diseased tissue can induce cytokinesis and release of growth factors that stimulate tissue repair. In addition, the tissue is promoted for differentiation along the required pathways.^[14] These discoveries have made MSCs an ideal origin for future cell therapies. In particular the adaptability to the exposed environment and the easy isolation procedure made MSCs a promising source for the treatment of diseases. Another important aspect of stem cell therapy is that the patients' own stem cells eliminate the risk of rejection by the immune system and the associated intake of immunosuppressive drugs, as MSCs have an anti-inflammatory effect on the surrounding tissue.^[15,16] In this study, mesenchymal stem cells are used in combination with fibrin-based hydrogels to investigate the influence of mechanical properties of a material on cells.

By modulating the mechanical and chemical properties of a fibrin-based matrix, human mesenchymal stem cells have been differentiated into osteoblasts and mouse embryonic stem cells have been triggered towards neural and astroglial lineages.^[17,18] Ye et al. have shown that fibrinolysis can be inhibited by the addition of aprotinin. They have also proven that cells in the fibrin gel grow homogeneous.^[19] Jockenhoevel et al. have also modified the fibrin gels via chemical border fixation with poly-L-lysine to prevent gel shrinking.^[20] The degradation rate of a fibrin gel can be regulated with aprotinin to precisely match tissue regeneration. Later, because aprotinin was associated with an increase of complications in clinical situations, tranexamic acid was used as an alternative.^[21] Though fibrin has been effective in vitro at promoting osteogenesis, it lacks the mechanical strength required for bone Tissue engineering

and in vivo studies have been disappointing even when a stiff scaffold encases the fibrin.^[22] Therefore, it is of high interest to modify fibrin gels to adjust their mechanical properties to meet the application criteria. The use of different buffers and different salt concentrations already influences fibrins' morphology and its mechanical properties.^[23] However, also the use of different additives is a promising approach to modulate the properties of fibrin. For example, in 2017 Jaspers et al. have shown, that it is possible to mimic the complex mechanical environment of cells by mixing polyisocyanopeptides with carbon nanotubes, fibrin, and polyacrylamide. They found out, that stiff, rod-like fibers show the stiffening behavior of semiflexible hydrogels while the addition of flexible polymers reduce the strain-stiffening.^[24] The addition of polyvinyl alcohol to fibrin gel resulted in hydrogels with an increased storage modulus G' , which means, that the gels are generally stiffer, and have an improved capability for rehydration.^[25] Other polymer-based additives were polyethylene glycol (PEG),^[26–28] PEG-based microgels with superparamagnetic iron oxide,^[27,29,30] hyaluronic acid,^[31] and copolymers based on (hydroxyethyl) methacrylate and *N*-hydroxysuccinimide methacrylate.^[32] All these approaches show how the hydrogel is influenced by the addition of synthetic polymers. They either show an increase in the storage modulus, the fiber orientation or the gels' stability.^[24–32]

In the present work, we develop a new concept to improve mechanical properties and slow down the degradation of fibrin hydrogels. This is achieved by the combination of reactive amphiphilic and biocompatible copolymers with fibrinogen and thrombin to fabricate composite hydrogels with tunable internal structure, adjustable mechanical properties, and degradation profiles. In addition, we demonstrate that new fibrin-based hydrogels exhibit no toxicity to cells and can regulate the cell proliferation.

2. Results and Discussion

In this work we synthesize hydrogels using fibrinogen, thrombin, and reactive amphiphilic copolymers based on *N*-vinyl lactams (Figure 1). *N*-vinyl lactam-based polymers show a good biocompatibility, have specific hydration properties, and exhibit lower critical solution temperature (LCST) in aqueous solutions.^[33] They can be easily synthesized via reversible addition–fragmentation chain transfer (RAFT) polymerization and copolymerization with different functional comonomers allowing for flexible variations of the chemical structure.^[34–38] The big advantage of RAFT, compared to other methods, is the biocompatibility of the polymerization type. While atom transfer radical polymerization (ATRP) is based on coordination chemistry of ligands with copper ions, RAFT dispenses with metal ions, which is of great importance for biomedical applications.^[39,40,41–48] We decide to use copolymers based on *N*-vinylpyrrolidone (VP) as main monomer and glycidyl methacrylate as comonomer based on the work of Peng et al. for the modification of the fibrin gels.^[38] The epoxy group of glycidyl methacrylate can bind covalently to thiol- and amine groups.^[50] Because of this property, our polymers develop covalent bonds with the amines and thiols in fibrinogen and the fibrin (Figure 1). The advantage is, that, because the covalent bonds are formed with amines in lysine residues, the plasmin cannot degrade the fibrin at these positions anymore.^[1] The

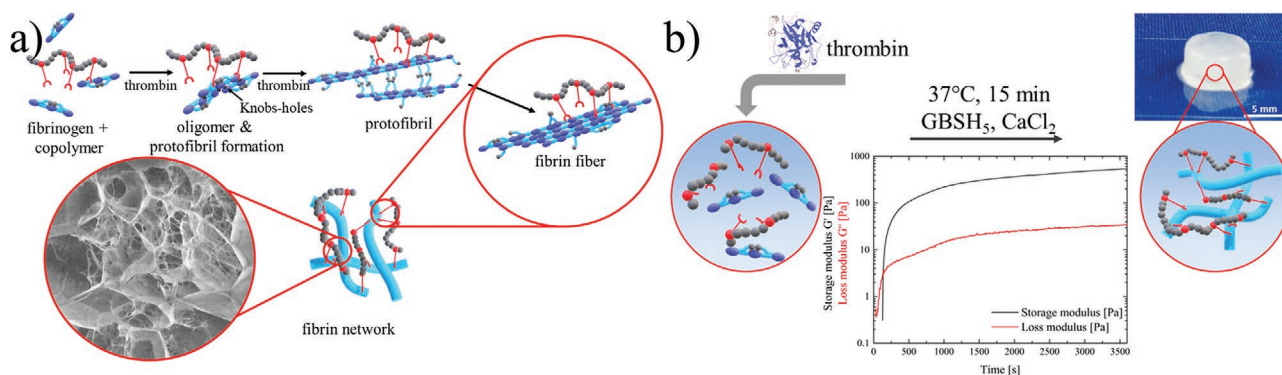


Figure 1. Scheme for the synthesis of fibrin-based hydrogels with a crosslinking copolymer. a) Formation of fibrin hydrogel from fibrinogen (blue rods) and a synthetic polymer (gray and red chain). The copolymers bind to the functional groups of the fibrinogen. Catalyzed by thrombin and via self-assembly protofibrils are formed. The protofibrils assemble to fibrin-fibers. b) Synthesis of hydrogels in lab scale. Fibrinogen and copolymers are in solution when thrombin is added (left). Hydrogel formation occurs at 37 °C within 15 min (middle). The used polymers lead to a double crosslinking of the hydrogel (right).

control hydrogel synthesis (fibrin without copolymers) is conducted as previously described.^[51–55]

2.1. Synthesis and Characterization of Reactive Copolymers

To analyze the influence of the PVP-*co*-GMA-copolymer on the hydrogel properties, copolymers with different molecular weights and different comonomer concentrations are synthesized. The intention is to analyze whether the increase of copolymers' molecular weight can induce a strain stiffening of the hydrogel. Apart from that, the GMA-amount and the polymer concentration have an influence on the hydrogel stiffness.

The copolymers are synthesized based on the works of Peng et al.^[38] via RAFT polymerization. The high molecular weight polymer is synthesized via free radical polymerization while the target molecular weight is adjusted via monomer to initiator ratio. The copolymers are characterized by NMR spectroscopy, GPC, and FTIR spectroscopy (Figures S1 and S2, Supporting Information). Since especially copolymers with low

concentrations of GMA are difficult to analyze with NMR, FTIR measurements are performed to evaluate the chemical composition of copolymers (Figure 2). PGMA- and PVP-homopolymers in different ratios and the intensity of the carbonyl absorption bands of the PGMA and the PVP from FTIR spectra are correlated to the real amounts of both polymers providing a calibration curve for the determination of the chemical composition of copolymers.

The equation which resulted from the obtained calibration curve is used to calculate the real amounts of the GMA in the PVP-*co*-GMA-polymers. The variables are defined as follows:

a (PGMA) = amount of PGMA in the copolymer [mol%]

h (X) = height of the carbonyl band in the FTIR-spectra of monomer X

Formula for the calculation of the PGMA amount

$$a(\text{PGMA}) = \frac{h - 0.02644}{1 + \frac{0.86031}{0.86031}} \cdot 100 \text{ with } h = \frac{h(\text{PGMA})}{h(\text{PVP})} \quad (1)$$

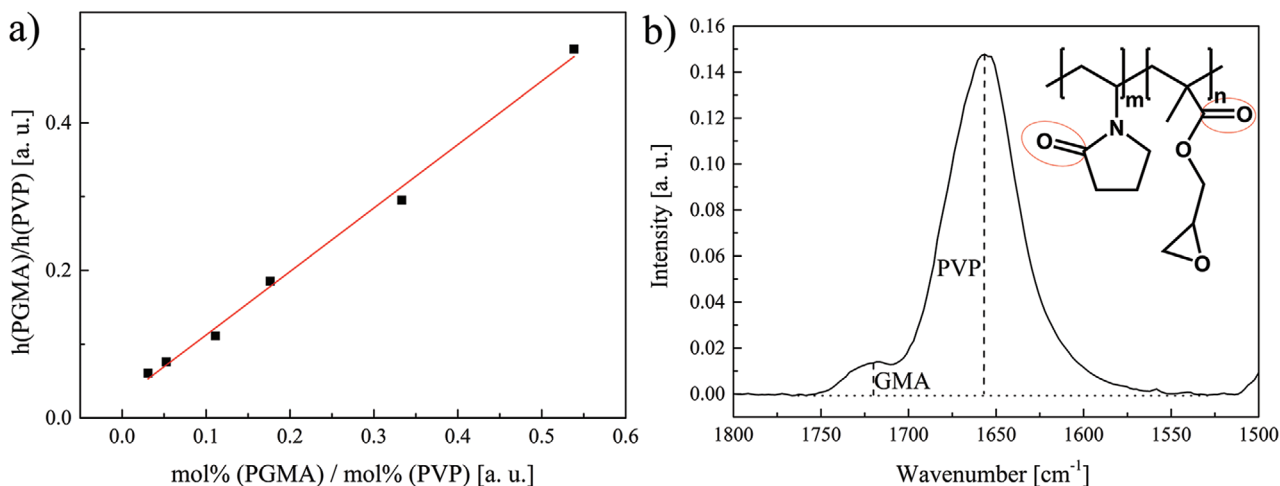


Figure 2. Characterization of the copolymer composition by FTIR spectroscopy. a) Calibration curve obtained from FTIR measurements showing the dependency of carbonyl bands ratio from PGMA and PVP composition in homopolymer mixture (intercept: 0.02644 ± 0.00821 , slope: 0.86031 ± 0.02969), b) part of the FTIR spectrum for copolymer PVP₁₆₄₀₀-*co*-GMA_{7mol%} showing carbonyl bands of GMA and VP (signal splitting can occur depending on the temperature during the FTIR measurement).

Table 1. Summary of the characterization of the copolymers.

No.	Sample name	GMA amount [mol%]	Mn [g mol ⁻¹]	Mw [g mol ⁻¹]	Dispersity, <i>D</i> [a. u.]
1	PVP ₁₁₁₀₀ - <i>co</i> -GMA _{3mol%}	3	11 100	13 900	1.25
2	PVP ₁₆₄₀₀ - <i>co</i> -GMA _{7mol%}	7	16 400	25 200	1.53
3	PVP ₅₇₀₀ - <i>co</i> -GMA _{9mol%}	9	5700	7000	1.24
4	PVP ₁₂₄₀₀ - <i>co</i> -GMA _{10mol%}	10	12 400	19 700	1.59
5 ^{a)}	PVP ₇₀₈₀₀ - <i>co</i> -GMA _{10mol%}	10	70 800	190 900	2.69
6	PVP ₁₇₀₀₀ - <i>co</i> -GMA _{11mol%}	11	17 000	24 400	1.44
7	PVP ₁₂₈₀₀ - <i>co</i> -GMA _{28mol%}	28	12 800	20 000	1.58

^{a)}Synthesized via free radical polymerization.

To analyze the real molecular weight of the copolymers GPC measurements are conducted. The results are summarized in **Table 1**.

The results show that the RAFT-synthesis for copolymers up to a molecular weight of 20 000 g mol⁻¹ was successful (dispersity between 1.2 and 1.6). The copolymers with GMA amounts of 9, 10 and 11 mol% are targeted with a GMA amount of 10 mol%. This means that also the targeted incorporation of the comonomer was successful. Due to the limitations of RAFT polymerization, the high molecular weight polymer (sample 5 in **Table 1**) is synthesized via free radical polymerization, which leads to a broader molecular weight distribution. In this synthesis the molecular weight is set via initiator to monomer ratio.

2.2. Synthesis of Hydrogels

The copolymer PVP₁₂₄₀₀-*co*-GMA_{10mol%} is selected for the analysis of the influence of the comonomer on the hydrogels' mechanical properties, because preliminary tests were promising for this molecular weight and comonomer concentration. The amounts of different ingredients used for the synthesis of hydrogels are shown in **Table 2**.

Table 2. Hydrogels synthesized with different fibrin:copolymer ratios (210 μL hydrogel contains 156 μL fibrinogen solution (40 mg mL⁻¹), 10 μL CaCl₂ solution (50 mM), 20 μL thrombin solution (20 U mL⁻¹), and 24 μL polymer solution).

Conc. polymer solution [mg mL ⁻¹]	Polymer amount in 24 μL polymer solution [mg]	Conc. fibrinogen solution [mg mL ⁻¹]	Fibrinogen amount in 156 μL solution [mg]	Amount copol- ymer compared to fibrinogen [wt%]
1	0.024	40	6.24	0.38
3	0.072	40	6.24	1.15
3.5	0.084	40	6.24	1.35
4.5	0.108	40	6.24	1.73
5	0.12	40	6.24	1.92
6	0.144	40	6.24	2.31
7	0.168	40	6.24	2.69
8.5	0.204	40	6.24	3.27
10	0.24	40	6.24	3.85

The variation of the copolymer concentration in the gelation mixture leads to the assumption, that the presence of copolymers influences the stiffness of the hydrogels. As shown in **Figure 3a**, there is an increase in the storage modulus observed up to an amount of 1.92 wt% copolymer. With a further increase of the copolymer amount, the storage modulus decreases again. We assume that at low concentration of copolymers with a low molecular weight (around 10 000 g mol⁻¹) the crosslinking of fibrin is not efficient. The assumption is that at low concentrations low molecular weight copolymers most probably become grafted on the fibrin fibers and form less "bridges" between them. In this case, no efficient reinforcement of hydrogels occurs. With an increase of the polymer concentration, it is possible to increase the amount of crosslinks between individual fibrin fibers. Since the copolymer is mixed with other components before the hydrogel formation starts, it is assumed that higher polymer amounts rather hinder the fiber formation than support the crosslinking of the fibers.

To analyze the amount of bonding types in the hydrogels, the storage and loss modulus are measured in dependence to the oscillation frequency (**Figure 3b**). Since the course is straight and not step like, only one bonding type is probable and we assume that the copolymer crosslinks the fibrin forming covalent bonds. It is known that in the basic medium epoxy groups react with amines or thiols which are present in the fibrin structure (**Figure 3d**).^[50]

A variation of the epoxy groups amount in the copolymer means also a variation of functional groups, which can potentially react with the functional groups in the fibrin fibers forming covalent bonds. The experimental results presented in **Figure 3c** demonstrate that with an increase of the GMA content in copolymers, an increase of the storage modulus occurs. The reference experiment performed with the PVP homopolymer of comparable molecular weight demonstrates that the formed hydrogel has a storage modulus similar to native fibrin indicating that reactive copolymers bind covalently to fibrin.

2.3. Variation of Molecular Weight

As low molecular weight copolymers only influenced the hydrogel stiffness by their concentration, measurements with copolymers of higher molecular weights are conducted. The focus is in this case on the targeted strain stiffening behavior (**Figure 4a**). Biopolymers in living organisms, like fibrin or collagen, show a specific strain stiffening behavior. The fibrin hydrogels produced in the vial show strain softening behavior. We want to analyze whether the copolymer can induce the strain stiffening behavior in fibrin hydrogels. While low molecular weight polymers are used, a higher stiffness of the hydrogel can be obtained, but there is no change in the strain-dependent behavior. **Figure 4b** shows storage moduli as a function of the oscillation strain for fibrin-based hydrogels synthesized with reactive copolymers exhibiting the same chemical composition but different molecular weights. It is obvious that native fibrin hydrogels show the increase of the storage moduli at oscillation strains above 100%. This effect is missing in fibrin-based hydrogels synthesized with copolymers of low and moderate molecular weights. However, the hydrogel sample

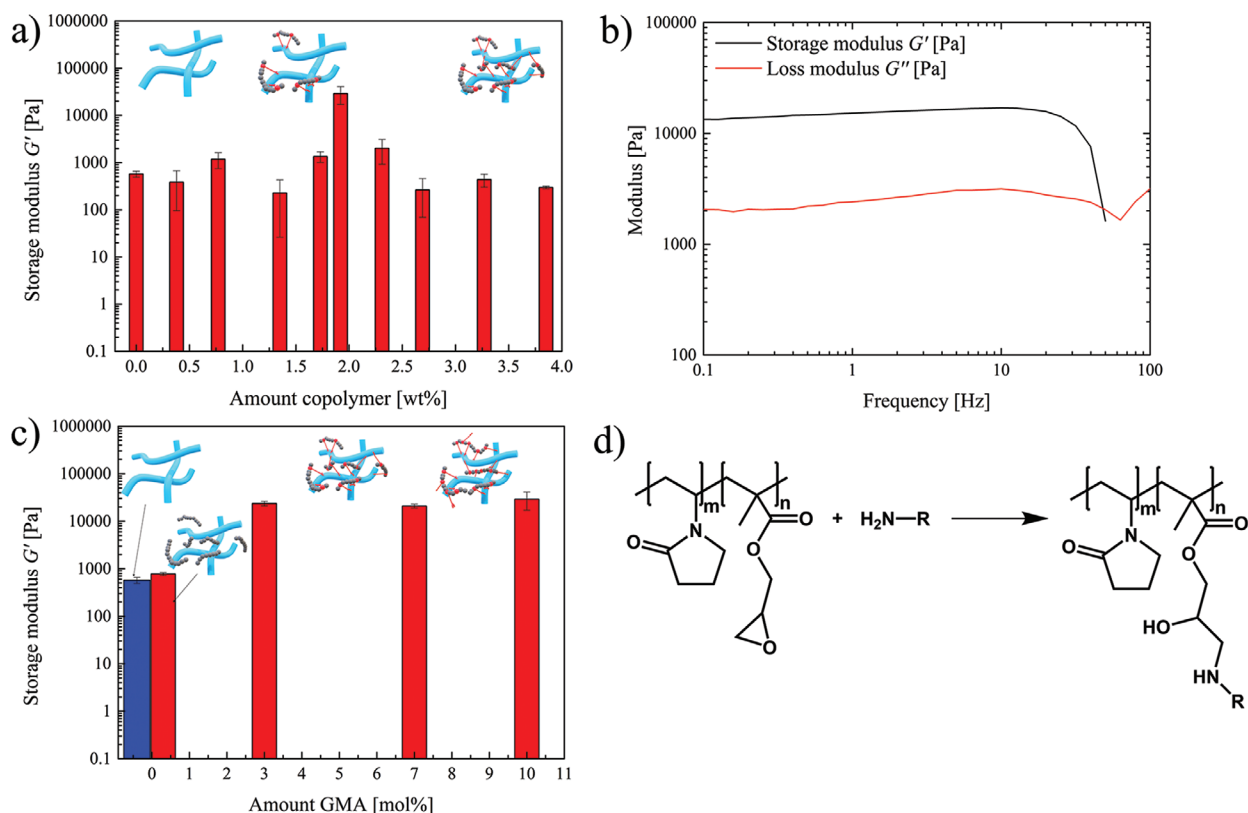


Figure 3. Rheological characterization of the hydrogels. a) Storage modulus (G') of fibrin-based hydrogels synthesized with different amounts of copolymer (PVP_{12400-co-GMA}_{10mol%}). b) Frequency-dependent measurement of storage G' and loss G'' moduli for hydrogel with 1.92 wt% PVP_{12400-co-GMA}_{10mol%}. c) Storage modulus G' for hydrogels synthesized with copolymers containing different amounts of epoxy groups (pure fibrin reference in blue). d) Reaction between the copolymer and an amine group of the fibrin.

synthesized with reactive copolymer of 70 800 g mol⁻¹ molecular weight shows very clear strain-stiffening behavior similar to native fibrin. At the same time this fibrin-based hydrogel sample exhibits higher storage moduli in the whole deformation range compared to native fibrin hydrogels indicating that

high molecular weight reactive copolymers induce strain stiffening because of an increased probability of fiber crosslinking.

To test whether the temperature-responsiveness of copolymers influences the temperature-dependent behavior of the hydrogels, rheological measurements at different temperatures are

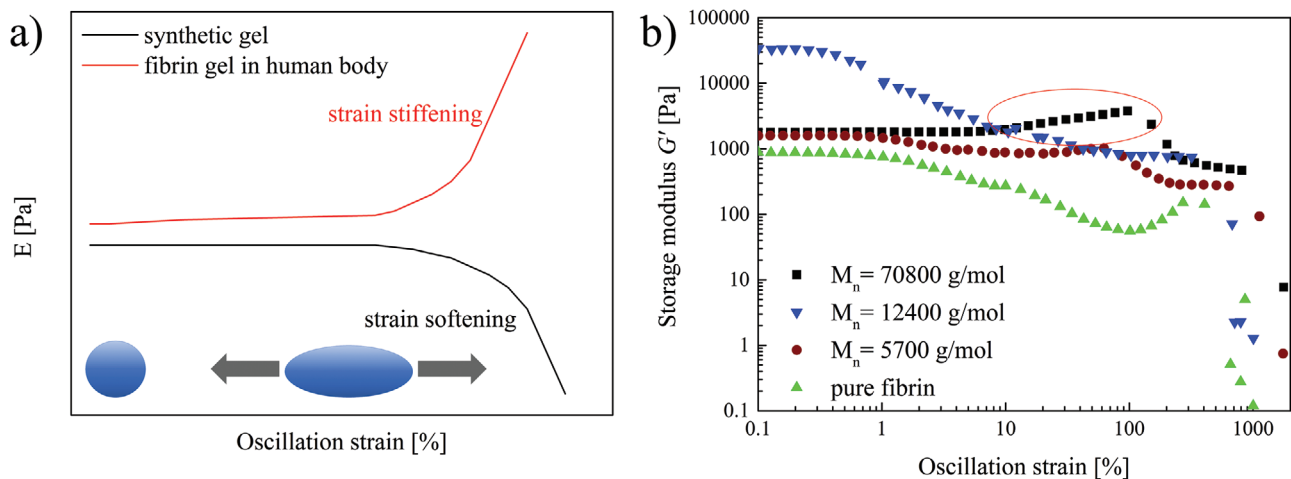


Figure 4. Analysis of strain-dependent behavior via rheology. a) General example for strain stiffening and strain softening behavior. b) Storage moduli as a function of oscillation strain for native fibrin and hybrid hydrogels synthesized with reactive copolymers of different molecular weights (GMA amount around 10 mol%, polymer concentration 1.92 wt%).

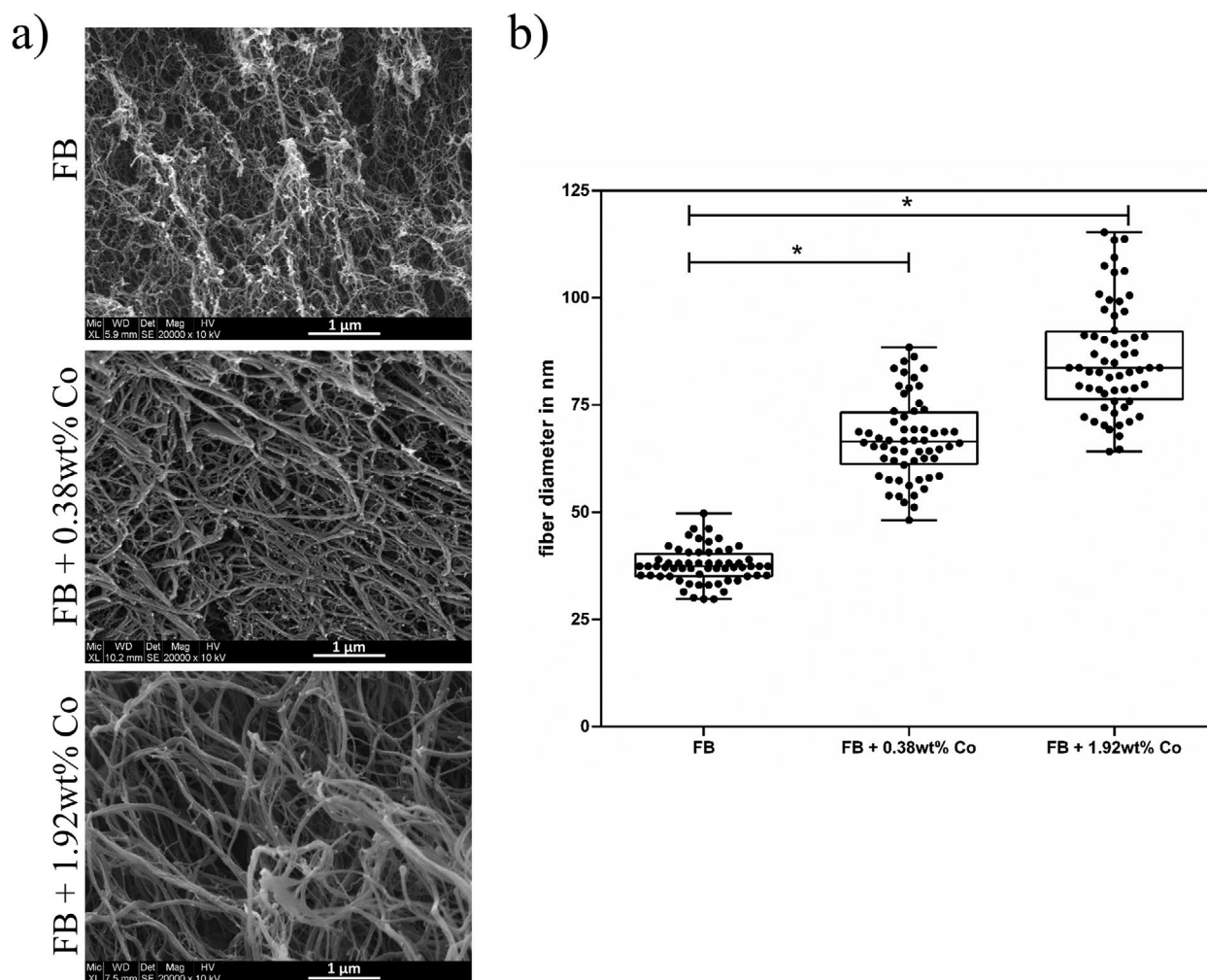


Figure 5. SEM analysis of fibrin hydrogels. a) SEM images of fibrin-based hydrogels synthesized with different concentrations of copolymers compared to fibrin hydrogels without copolymers. Due to the increasing concentration of copolymers, an increase in fiber thickness is observed. (magnification: 20 000 \times , Scale bar: 1 μ m). b) Determined average fiber diameters for different fibrin hydrogels ($p^* < 0.01$, FB = Fibrin).

conducted (Figure S3, Supporting Information). All hydrogels show a higher storage modulus because a new batch of fibrinogen is used. Similar to the previous measurements the copolymer PVP₁₂₄₀₀-*co*-GMA_{10mol%} with a concentration of 1.92 wt% is used. It is found that hydrogels show similar mechanical properties at temperatures above and below lower critical solution temperature (LCST) of reactive copolymer. The reason for this is probably the low copolymer concentration in the hydrogel, which may induce some local changes in the network topology and water content but has no impact on the bulk properties of hydrogels.

2.4. Influence of Polymer Concentration on Fibrin Fiber Thickness

In order to investigate how the different concentrations of the reactive copolymers influence the morphology of the fibrin fibers, we select copolymer sample 4 (PVP₁₂₄₀₀-*co*-GMA_{10mol%}) and synthesize hydrogels with copolymer concentrations of 0.38 and 1.92 wt% relatively to the fibrinogen amount. For each hydrogel composition, six samples are synthesized to ensure

the reproducibility of the results. The morphology of fibers in hydrogels is analyzed with scanning electron microscopy (SEM) and after the image acquisition, the fiber thickness is evaluated with Scandium imaging software (Figure 5a). For the determination of the average fiber thickness, ten fibrin fibers are measured manually from each fibrin hydrogel (Figure 5b). The results show a significant ($p^* < 0.01$) increase in fiber diameter for hydrogels prepared with 0.38 and 1.92 wt% copolymer compared to fibrin hydrogels without copolymer. Fibrin fibers have diameters of 25–50 nm, and with the addition of the copolymer, the diameter increased to an average of 67 and 85 nm. These experimental results confirm our hypothesis that reactive copolymers interact actively with fibrinogen during the gelation process forming covalent bonds with proteins, what increases the thickness of the fibrin fibers. In addition, the SEM images of hydrogels synthesized in the presence of reactive copolymers indicate a clear formation of bridges between individual fibrin fibers. The abovementioned effects, increase of the fiber thickness, and formation of inter-fiber crosslinks, improves the mechanical properties of fibrin-based hydrogels.

2.5. Cell Viability and Cytotoxicity

For the later application of the copolymer *in vitro*, it is of particular importance to exclude cytotoxic behavior, especially from epoxy groups present in the copolymer structure. First of all, a cytotoxicity test according to ISO 10993-5 is performed and the results obtained are confirmed by a separate cell viability assay (CellTiter-Blue, Promega, Mannheim, Germany).

2.5.1. Cytotoxicity/Viability Test According to ISO 10993-5

Live/dead stainings are performed with L929 mouse fibroblasts and human mesenchymal stem cells (MSC) on TCPS, fibrin, and fibrin-based hydrogels in combination with 0.38 and 1.92 wt% of copolymer 4 (Table 1). Cells are cultured for 1, 3, and 7 days. The results (Figure 6a) show no significant difference over the whole culture period between fibrin and fibrin-based hydrogels with different copolymer concentrations, neither for L929 cells nor for MSC. Cell morphology is comparable to control conditions on TCPS for both cell types. L929 fibroblasts show an increase in cell proliferation when cultured on fibrin gels with and without copolymer. This can be explained by the softer ECM provided by the hydrogels. Images are quantified with ImageJ and the percentage of dead cells is calculated by the ratio of dead and living cells (Figure 6b). Due to the increased proliferation rate and thus post-confluent growth of

L929 mouse fibroblasts, only the first 3 days can be statistically evaluated. No significant differences can be observed between TCPS, fibrin, and fibrin-based hydrogels with addition of copolymers. The average percentage of dead cells is less than 1% for each condition with both cell types. An increase in cytotoxicity over a period of 3 days for L929 cells and 7 days for MSC is not detected. The results can be used to predict a cytocompatible behavior of the used copolymers *in vivo*. To confirm these results, an additional viability test is performed.

2.5.2. Cell Viability (CellTiter-Blue)

Cell viability is measured using the CellTiter-Blue Cell Viability Assay. The results are normalized to day 1. L929 mouse fibroblasts show an increase in cell proliferation when cultured on fibrin-based hydrogels (Figure 7). Fibrin without the addition of copolymers has a significant impact on viability and proliferation of L929 cells, compared to the TCPS control. With addition of 0.38 and 1.92 wt% of copolymer number 4 with 10% GMA content (Table 1), proliferation rate decreased but is overall higher than the control group. Stiffness of the surrounding material can affect proliferation rate and due to an increase of storage modulus when higher copolymer concentrations are added into the fibrin-based hydrogel, this can be attributed to an increased proliferation. Human mesenchymal stem cells show no significant increase in cell viability/proliferation at

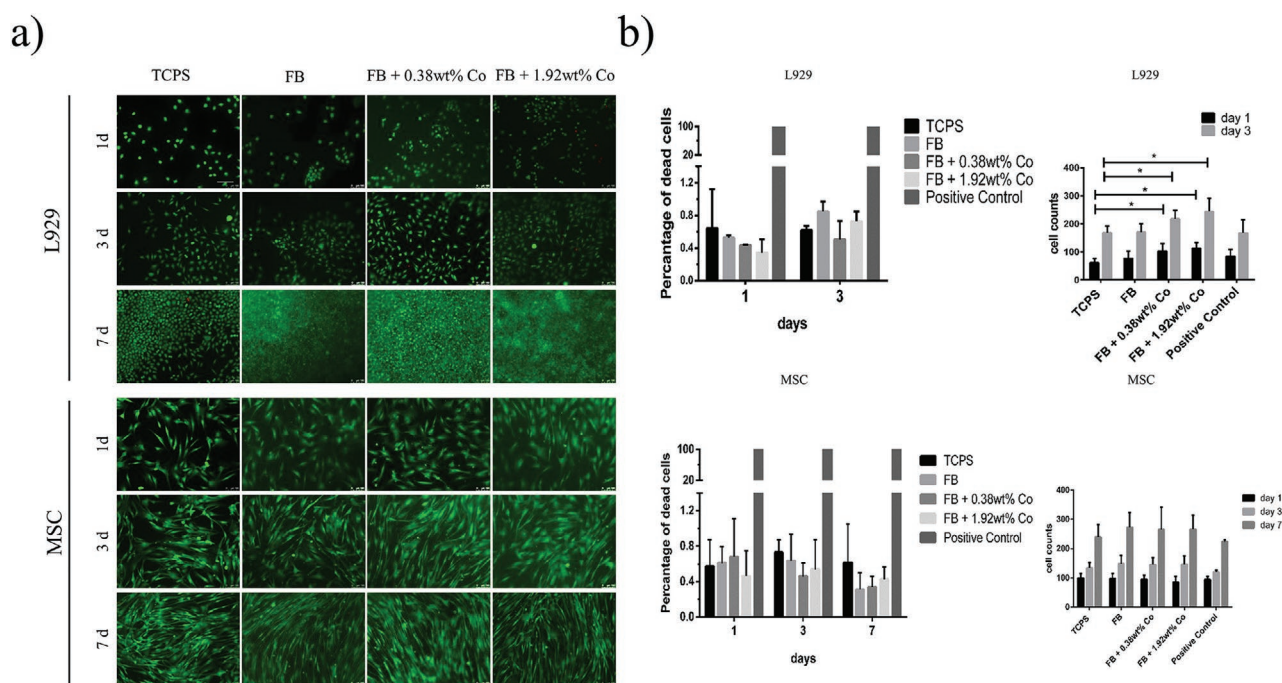


Figure 6. Live/dead stainings of different cell types on fibrin-based hydrogels with and without copolymers. a) Cytotoxicity test of fibrin-based hydrogels in combination with different copolymer concentrations according to ISO-10993-5. L929 cells and MSC are cultured for 1, 3, and 7 days on the hydrogels. Live/dead stainings demonstrate viable cells by green fluorescence and dead cells by red fluorescence. Morphology of L929 cells as well as MSC is characteristic for the respective cell type on fibrin-based hydrogels with the addition of various amounts of copolymer. Magnitude: 100 \times , Scale: 100 μ m. b) Statistical evaluation of live/dead stainings of L929 cells and MSC on fibrin-based hydrogels with different concentrations of copolymers and corresponding cells. Percentage of dead cells is calculated by comparing the ratio of viable and dead cells. No cytotoxicity can be detected, neither for fibrin nor for fibrin-based hydrogels with the addition of different copolymer concentrations. The cell count has increased over time and a significant rise in L929 cells on days 1 and 3 was demonstrated at both copolymer concentrations when compared with the TCPS control (FB = Fibrin, Co = Copolymer).

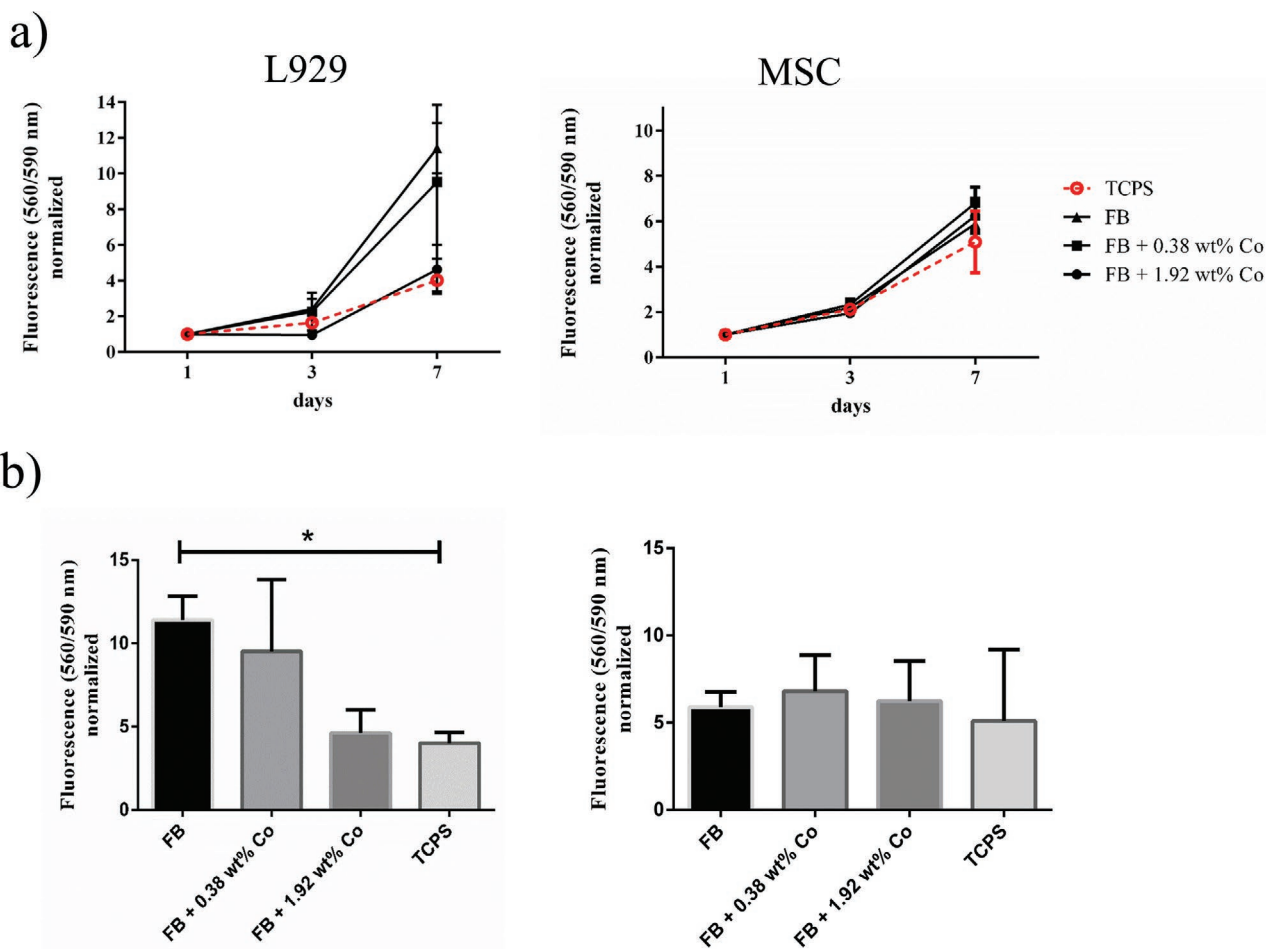


Figure 7. Viability assay of different cell types on fibrin and fibrin-based hydrogels. a) CellTiter-Blue Cell Viability Assay is performed after 1, 3, and 7 days. L929 mouse fibroblasts and MSC are seeded on TCPS, FB, and FB with different copolymer concentrations. Fluorescent resorufin was detected at 560/590 nm and normalized to day 1. b) Results of CellTiter-Blue Cell Viability Assay for L929 cells and MSC after 7 days in culture with TCPS, FB, and FB with different copolymer concentrations are shown. Significant increase ($p^* < 0.01$) in cell proliferation is detected on FB compared to TCPS. L929 fibroblasts show an overall increased proliferation rate when cultured on fibrin hydrogels. For the proliferation rate of MSC, no significant differences to the control conditions are detectable (FB = Fibrin, Co = Copolymer).

each given time point. The overall proliferation rate is comparable to the TCPS control.

2.6. Human D-Dimer ELISA

Human D-Dimer ELISA is performed to evaluate whether the used copolymer can reduce the rate of fibrinolysis through MSC and thus lead to a controlled degradation of the fibrin-based hydrogels. D-Dimers are fibrinolytic peptides as a result of fibrin degradation. No tranexamic acid is used, to allow for physiological fibrinolysis. The standard curve (Figure S4a, Supporting Information) is created according to the manufacturers' specifications, with measured D-Dimer concentrations in the range from 0.1–1000 pg mL^{-1} . Resulting determination coefficient equals 0.9985. Results indicate that the addition of a higher weight percentage of copolymer inhibits fibrinolytic processes and therefore a controlled degradation of fibrin-based hydrogels can be ensured (Figure 8). Hydrogels cultured

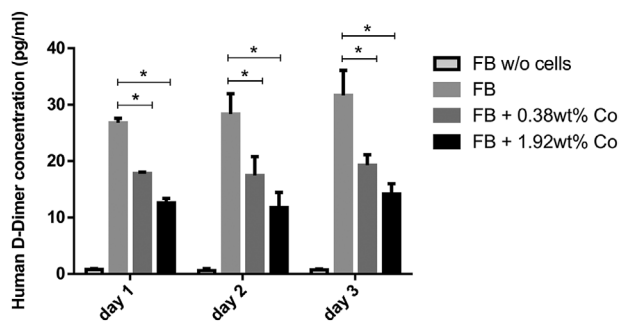


Figure 8. Decrease of fibrin degradation through addition of higher copolymer concentrations in fibrin-based hydrogels analyzed by human D-Dimer ELISA. Results of performed D-Dimer ELISA show a significantly reduced amount of D-Dimer concentrations ($p^* < 0.01$) for fibrin-based hydrogels which are prepared with additional copolymer. Cells are cultured for 1–3 days on fibrin-based hydrogels and TCPS. With increased copolymer concentrations, a decreased D-Dimer concentration is detected at each time point. No degradation of fibrin is detectable in absence of MCS.

without MSC show low amounts of D-Dimers ($<1 \text{ pg mL}^{-1}$). In contrast, the amount of D-Dimers present in the supernatant increased over time, when fibrin-based hydrogels are cultured without addition of copolymers (26.77, 28.37, and 31.63 pg mL^{-1}). By adding 0.38 or 1.92 wt% of copolymer, D-Dimer concentration can significantly ($p^* < 0.1$) decrease and remain stable over time, compared to FB. By comparing the two copolymer concentrations, it can be concluded that the D-Dimer concentration in the medium is reduced by 30% for 1.92 wt% copolymer. To ensure efficiency of the fibrinolysis inhibitor, the D-Dimer ELISA is also carried out with the addition of tranexamic acid (Figure S4b, Supporting Information).

Summarizing the experimental results presented above, one big advantage of PVP-co-GMA copolymers, compared to other linear polymers is, that at higher molecular weights PVP-co-GMA copolymers induce the strain stiffening behavior of the hydrogels.^[24] In addition, the hydrogel preparation with this copolymer is simple and the gelation mixture is easy to handle. The polymer does not have to be further modified like polyvinyl alcohol to interact specifically with fibrin. Apart from that, the modified polyvinyl alcohol needs addition of a photoinitiator to crosslink efficiently.^[25] Also PEGylated fibrinogen needs a photoinitiator and irradiation for a successful modification of the hydrogel.^[26] It has been demonstrated that PEG can also be modified with peptides derived from antiplasmin to reduce the degradation. In this work we demonstrate that the degradation of the fibrin-based hydrogels can be strongly retarded without coupling with peptides.^[28] Polyvinyl amine is also used in literature for fibrin modification, but, compared to PVP-co-GMA, it shows a lower viability of cells.^[25] Additionally, vinyl pyrrolidone can be synthesized from glutamic acid, which is a by-product of biofuel production.^[56–58] When this synthesis will be used for the commercial production of vinyl pyrrolidone, bio-based PVP-co-GMA copolymers can be synthesized.

3. Conclusion

In the present work, we developed a new concept to synthesize fibrin-based hydrogels with improved mechanical properties and retarded degradation. This was achieved by the combination of reactive amphiphilic and biocompatible copolymers with fibrinogen and thrombin to fabricate composite hydrogels. We demonstrate that using these building blocks it is possible to fabricate hydrogels with tunable internal structure, adjustable mechanical properties, and degradation profiles. The increase of the reactive copolymer concentration in the reaction mixture up to 2 wt% increases the storage modulus of fibrin-based hydrogels. It is also possible to induce strain stiffening of hydrogels by the regulation of molecular weight of the copolymer. Investigating the internal structure of hydrogels, we found that the thickness of the fibrin fibers in hydrogels increases with the increase of copolymer concentration. First in vitro results demonstrate no cytotoxic effects of the chosen copolymer on L929 mouse fibroblast and human mesenchymal stem cells (MSC). Furthermore, the use of this specific copolymer can lead to significantly slower degradation of fibrin hydrogels in vitro, which makes the use of fibrinolytic inhibitors, such as tranexamic acid, no longer necessary. This can be particularly advantageous

for the in vivo applications of fibrin-based hydrogels as implant coatings.

4. Experimental Section

Materials: If not mentioned otherwise, all materials were used without additional purification. *N*-vinylpyrrolidone was purchased from TCI chemicals and distilled before use to remove the inhibitor. Glycidyl methacrylate (GMA) was purchased from Sigma-Aldrich and was also distilled before use. The azobisisobutyronitrile (AIBN) was purchased from Sigma-Aldrich and recrystallized in methanol before use. Methyl 2-bromopropionate (98% purity) and potassium ethyl xanthogenate (96% purity) were purchased from Sigma-Aldrich. Fibrinogen from human plasma (35–65% protein), thrombin from human plasma ($\geq 1000 \text{ NIH units mg}^{-1}$ protein), HEPES sodium salt (suitable for cell culture), sodium phosphate dibasic ($\geq 99\%$ purity), magnesium sulfate heptahydrate ($\geq 99\%$ purity) were purchased from Sigma-Aldrich. All used organic solvents were practical or HPLC grade.

Synthesis of Chain Transfer Agent: The RAFT agent Rhodixan A1 was synthesized as already described in the literature.^[59] First, in a double-neck flask, methyl 2-bromopropionate (40 g, 234 mmol, 1 equiv.) was dissolved in ethanol (300 mL) and stirred under cooling with ice. Then, potassium ethyl xanthogenate (43.1 g, 268 mmol, 1.1 equiv.) was stepwise added as a powder to the solution over 45 min and then stirred for 3 h at room temperature. For the workup the solution was filtered and concentrated at $40 \text{ }^\circ\text{C}$ under a pressure of 175 mbar. After the addition of dichloromethane (600 mL) the organic phase was extracted with distilled water ($4 \times 100 \text{ mL}$) and dried over magnesium sulfate for 12 h. The drying agent was removed via filtration. The dichloromethane was removed under reduced pressure. The RAFT agent was dried under vacuum for 8 h. The product was a clear, bright yellow liquid (yield = 92%).

Synthesis of PVP-co-PGMA-Copolymers via RAFT Polymerization: The polymer synthesis was performed based on the work of Peng et al.^[38] The reaction was performed under inert atmosphere. The amounts of the substrates were shown for a target molecular weight (M_n) of $10\,000 \text{ g mol}^{-1}$ and a GMA amount of 3 mol%. First, VP (4.0 g, 36 mmol, 1 equiv.) and the CTA (0.043 g, 0.21 mmol) were dissolved in anisole (6 mL) and degassed in a Schlenk-flask with five freeze-pump-thaw-cycles. The vials with the GMA (0.15 g, 1.08 mmol, 0.03 equiv.), dissolved in anisole (2 mL), and the initiator (AIBN, 0.0068 g, 0.042 mmol, 0.0012 equiv.), also dissolved in anisole (0.4 mL), were purged with nitrogen under ice cooling for 30 min. At $60 \text{ }^\circ\text{C}$ the solution with the initiator was added to the reaction, to start the polymerization. The GMA was added continuously, with a rate of 0.15 mL h^{-1} , to the reaction flask via a syringe pump. After 24 h the reaction was stopped by cooling the mixture in liquid nitrogen. The product was precipitated in cold diethyl ether (400 mL) and dried under vacuum at $40 \text{ }^\circ\text{C}$ for 36 h (yield = 88%).

Hydrogel Preparation: The polymer was dissolved in different concentrations in GBSH₅-buffer (0.37 g L⁻¹ KCl, 0.2 g L⁻¹ MgCl₂ in 6H₂O, 0.15 g L⁻¹ MgSO₄ in 7H₂O, 7.00 g L⁻¹ NaCl, 0.12 g L⁻¹ Na₂HPO₄, 1.19 g L⁻¹ HEPES). Fibrinogen (156 μL , 40 mg mL⁻¹ in GBSH₅-buffer), CaCl₂-solution (10 μL , 50 mM), and the polymer solution (24 μL) were mixed in a vial at $0 \text{ }^\circ\text{C}$. Then, thrombin (20 μL , 20 U mL⁻¹) was added. The solution was shaken and incubated at $37 \text{ }^\circ\text{C}$ for at least 20 min. A turbid, solid hydrogel was obtained.

Scanning Electron Microscopy: In order to investigate the effects of the fibrin-binding copolymers on the individual fibrin fibers, the gels were examined using scanning electron microscopy. The fibrin-based hydrogels were poured into a 96-well plate. First, 10 μL thrombin (20 U mL⁻¹) was pipetted into a well and then mixed with the fibrin-copolymer-solution. Each condition was prepared six times to investigate the reproducibility of the hydrogels. After the gels were polymerized, they were stored overnight in medium at $37 \text{ }^\circ\text{C}$, then fixed with 2.5% glutaraldehyde in PBS, and stored at $4 \text{ }^\circ\text{C}$ until further preparation. The samples were rinsed with 0.1 M

sodium phosphate buffer (pH 7.39, MERCK, Darmstadt, Germany) and dehydrated by incubation in an ascending ethanol series (30%, 50%, 70%, and 90%) with a final incubation of three times in 100% ethanol for 10 min. The constructs were then critical-point-dried in liquid CO₂ (Quorum Technologies, Ashford, United Kingdom), and coated with a 10 nm gold/palladium layer (Sputter Coater EM SCD500, Leica, Wetzlar, Germany). The samples were ripped open and the microscopy was performed in a high vacuum environment at 10 kV acceleration voltages with an environmental scanning electron microscope (ESEM XL30 FEG, FEI, Eindhoven, The Netherlands). Quantification of fibrin fibers was performed with the provided SEM Software Scandium. For evaluation, ten fibers were measured from each fibrin hydrogel.

Rheological Characterization: The used instrument is a TA Instrument Discovery HR-3 hybrid rheometer with a 20 mm cone-plate geometry which has a cone angle of 2°. It induces a sinusoidal shear deformation. The hydrogel was synthesized as described before but instead of the incubation, a volume of 74 µL was put in the rheometer, which was heated to a temperature of 37 °C. To ensure that the hydrogel is fully polymerized, a time-dependent measurement at a frequency of 1 Hz and an oscillation strain of 0.1 % was performed. Then, a frequency-dependent measurement at a fixed oscillation strain of 0.1% was conducted. The characterization was finalized with a strain-dependent measurement at a fixed frequency of 1 Hz.

Cell Culture: Cell culture experiments were approved by the local Ethics Committee (EK300/13). Human tissue donations were received with informed consent. All cells were cultured in a 20% O₂ and 5% CO₂ humidified atmosphere at 37 °C. All cells were tested for possible mycoplasma contaminations prior to the experiments.

L929 Mouse Fibroblast Cell Line: L929 mouse fibroblasts (ATCC, Wesel, Germany) were cultured in Roswell Park Memorial Institute (RPMI) 1640 medium (Gibco, Darmstadt, Germany) supplemented with 5% newborn calf serum (NCS, Gibco, Darmstadt, Germany), 1% penicillin (80 U mL⁻¹, Gibco, Darmstadt, Germany), 1% streptomycin (80 µg mL⁻¹, Gibco, Darmstadt, Germany), and 1% L-glutamine (1.6 mM, Gibco, Darmstadt, Germany).

Human Mesenchymal Stem Cells: Human mesenchymal stem cells (MSC) were isolated according to protocols from Pittenger et al.^[60] and Haynesworth et al.^[61] In brief, femoral heads of patients with total hip endoprosthesis (TEP) were surgically removed with informed consent of the affected patients and provided by the Orthopaedic Clinics of the University Hospital RWTH Aachen University. Bone marrow spongiosa was rinsed with stem cell medium (Mesenpan, PanBiotech, Aidenbach, Germany) several times and the remaining cell suspension was centrifuged for 10 min at 250 g. Subsequently, the supernatant was aspirated and the cell sediment was resuspended in 10 mL phosphate-buffered saline (PBS) and centrifuged for 10 min at 250 g. Afterward, the cell pellet was resuspended in stem cell medium and cells were seeded in a T75 culture flasks (Cellstar, Greiner bio-one, Frickenhausen, Germany). After 24 h of incubation, the medium was removed and the cells were washed twice with 10 mL PBS to get rid of non-adherent (hematopoietic) cells, bone fragments, and erythrocytes and a medium change was performed. Mesenchymal stem cells were expanded in Mesenpan (Pan-Biotech, Aidenbach, Germany) which contains 2% fetal calf serum (Pan-Biotech, Aidenbach, Germany), 1% ITS-plus (insulin–transferrin–selenic acid and bovine serum albumin (BSA)–linoleic acid (Pan-Biotech, Aidenbach, Germany), 1 nM dexamethasone (Pan-Biotech, Aidenbach, Germany), 100 µM ascorbic acid-2-phosphate (Pan-Biotech, Aidenbach, Germany), 10 ng mL⁻¹ epidermal growth factor (EGF, Pan-Biotech, Aidenbach, Germany), 1% penicillin (80 U mL⁻¹, Gibco, Darmstadt, Germany), 1% streptomycin (80 µg mL⁻¹, Gibco, Darmstadt, Germany), and 1% L-glutamine (1.6 mM, Gibco, Darmstadt, Germany). Medium was changed every 3–4 days. At 80–90% confluence, stem cells were trypsinized with 0.01% trypsin (Lonza, Cologne, Germany) and reseeded in a density of 5 × 10³ cells cm⁻². Cells were characterized by flow cytometry.

Viability/Cytotoxicity Test According to ISO 10993-5: To detect cytocompatibility and cytotoxicity of the produced copolymers in combination with fibrin, a live/dead staining of stem cells on the material was performed after 1, 3, and 7 days after seeding, according to the

protocols 10993–5 of the International Standardization Organization (ISO). Briefly, 1.2 mL Ringer solution (B. Braun, Melsungen, Germany) was mixed with 10 µL fluoresceindiacetat (FDA, 5 mg mL⁻¹ in acetone, Sigma-Aldrich, Steinheim, Germany) and 10 µL propidiumiodid (PI, 0.5 mg mL⁻¹ in PBS, Sigma-Aldrich, Steinheim, DE) and added to the cells, which were seeded on fibrin-based hydrogels and analyzed using fluorescence microscopy (DMI6000B, Leica, Wetzlar, Germany). Green fluorescence indicates viable cells and red fluorescence dead cells. To produce dead cell controls, 20 µL Triton-X100 (0.1% dissolved in PBS, Sigma-Aldrich, Steinheim, Germany) was added to lyse the cells. Quantification of the images was performed by ImageJ software.

Due to different cell sizes, the cell seeding density is cell type-dependent: 1.5 × 10⁴ cells cm⁻² for MSC and 1.8 × 10⁴ cells cm⁻² for L929 mouse fibroblasts.

Cell Viability (CellTiter-Blue): The CellTiter-Blue Cell Viability Assay (Promega, Mannheim, Germany) provides a homogeneous, fluorescent method for monitoring cell viability. The assay is based on the ability of living cells to convert a redox dye (resazurin) into a fluorescent end product (resorufin). Non-viable cells rapidly lose metabolic capacity and thus do not generate a fluorescent signal. Cells were seeded on fibrin-based hydrogels in 96-well plates (Falcon, Kaiserslautern, Germany). Cell densities are cell type-specific (1.5 × 10⁴ cells cm⁻² for MSC, 1.8 × 10⁴ cells cm⁻² for L929 cells). Every well was filled with 120 µL of the corresponding cell suspension and the assay was performed after 1, 3, and 7 days. The assay plates were taken out of the incubator, medium was removed from each well, and 20 µL of CellTiter-Blue Reagent were added and the plate was being shaken manually for about 10 s to distribute the reagents in the wells. The cells were then incubated for 3 h using the standard cell culture conditions. Afterward, the supernatant was transferred into a black 96-well plate and the fluorescence was measured at 560 nm excitation and 590 nm emission (Infinite M200 Reader, Tecan, Männergdorf, Switzerland). Fibrin gels without cells were incubated in parallel to serve as negative controls (background fluorescence). The assay was performed in triplicates.

D-Dimer Human ELISA: Human D-Dimer enzyme-linked immunosorbent assay (ELISA, Thermo Scientific, Dreieich, Germany) was performed according to the manufacturers' instructions. In previous experiments, tranexamic acid (16 µL mL⁻¹) was added to the cell culture in order to inhibit fibrinolysis by MSC^[62] and the associated digestion of the fibrin-based hydrogel. To evaluate the potency of the copolymer to inhibit fibrin degradation processes, the test setup was carried out with and without tranexamic acid. Human MSCs were seeded in a density of 1.5 × 10⁴ cells cm⁻² and medium was collected from the samples after 1, 2, and 3 days in culture. Used samples were diluted 1:100 with provided assay diluent.

Supporting Information

Supporting Information is available from the Wiley Online Library or from the author.

Acknowledgements

M.A.A.E.-U., H.M., S.N., and A.P. contributed equally to this work. This work was supported by the Deutsche Forschungsgemeinschaft (DFG) in the framework of the joint project “Towards a model-based control of biohybrid implant maturation” (PAK961) by the grant NE1650/4-1 and PI614/13-1. The authors acknowledge Karl Martin Graff for doing pretests with different molecular weight copolymers in the used system. The authors also acknowledge Bea Becker for conducting FTIR measurements. The authors thank the Clinic for Orthopedic Surgery for providing bone spongiosa to isolate human mesenchymal stem cells.

Conflict of Interest

The authors declare no conflict of interest.

Keywords

hierarchical structures, hybrid materials, hydrogels, medical applications, tissue engineering

Received: April 22, 2020

Revised: May 27, 2020

Published online: July 21, 2020

- [1] J. W. Weisel, in *Advances in Protein Chemistry*, Vol. 70 (Eds: D. A. D. Parry, J. M. Squire), Academic Press, London **2005**, pp. 247–299.
- [2] A. M. Carter, K. F. Standeven, P. J. Grant, in *Emery and Rimoin's Principles and Practice of Medical Genetics* (Eds: D. L. Rimoin, R. E. Pyeritz, B. Korf), Academic Press, Cambridge, MA **2013**, pp. 1–20.
- [3] J. W. Weisel, *Biophys. Chem.* **2004**, *112*, 267.
- [4] K. Bailey, W. T. Astbury, K. M. Rudall, *Nature* **1943**, *151*, 716.
- [5] J. W. Weisel, R. I. Litvinov, *Subcell. Biochem.* **2017**, *82*, 405.
- [6] C. Storm, J. J. Pastore, F. C. MacKintosh, T. C. Lubensky, P. A. Janmey, *Nature* **2005**, *435*, 191.
- [7] O. W. Petersen, L. Ronnov-Jessen, A. R. Howlett, M. J. Bissell, *Proc. Natl. Acad. Sci. U. S. A.* **1992**, *89*, 9064.
- [8] H. Liu, K. Roy, *Tissue Eng.* **2005**, *11*, 319.
- [9] J. P. Winer, S. Oake, P. A. Janmey, *PLoS One* **2009**, *4*, e6382.
- [10] Y. Li, H. Meng, Y. Liu, B. P. Lee, *Sci. World J.* **2015**, *2015*, 685690.
- [11] N. Joyce, G. Annett, L. Wirthlin, S. Olson, G. Bauer, J. A. Nolte, *Regener. Med.* **2010**, *5*, 933.
- [12] Y. Jiang, D. Henderson, M. Blackstad, A. Chen, R. F. Miller, C. M. Verfaillie, *Proc. Natl. Acad. Sci. U. S. A.* **2003**, *100*, 11854.
- [13] P. Trivedi, N. Tray, T. Nguyen, N. Nigam, G. I. Gallicano, *Stem Cells Dev.* **2010**, *19*, 1109.
- [14] J. M. Gimble, A. J. Katz, B. A. Bunnell, *Circ. Res.* **2007**, *100*, 1249.
- [15] A. Farin, C. Y. Liu, I. A. Langmoen, M. L. J. Apuzzo, *Neurosurgery* **2009**, *65*, 831.
- [16] R. M. Richardson, A. Singh, D. Sun, H. L. Fillmore, D. W. Dietrich, M. R. Bullock, *J. Neurosurg.* **2010**, *112*, 1125.
- [17] S. M. Willerth, K. J. Arendas, D. I. Gottlieb, S. E. Sakiyama-Elbert, *Biomaterials* **2006**, *27*, 5990.
- [18] I. Catelas, N. Sese, B. M. Wu, J. C. Y. Dunn, S. Helgersson, B. Tawil, *Tissue Eng.* **2006**, *12*, 2385.
- [19] Q. Ye, G. Zünd, P. Benedikt, S. Jockenhoevel, S. P. Hoerstrup, S. Sakiyama, J. A. Hubbell, M. Turina, *Eur. J. Cardio-Thoracic Surg.* **2000**, *17*, 587.
- [20] S. Jockenhoevel, G. Zund, S. P. Hoerstrup, K. Chalabi, J. S. Sachweh, L. Demircan, B. J. Messmer, M. Turina, *Eur. J. Cardio-Thoracic Surg.* **2001**, *19*, 424.
- [21] E. Cholewinski, M. Dietrich, T. C. Flanagan, T. Schmitz-Rode, S. Jockenhoevel, *Tissue Eng., Part A* **2009**, *15*, 3645.
- [22] U. Kneser, A. Voogd, J. Ohnolz, O. Buettner, L. Stangenberg, Y. H. Zhang, G. B. Stark, D. J. Schaefer, *Cells Tissues Organs* **2005**, *179*, 158.
- [23] N. A. Kurniawan, T. H. S. Van Kempen, S. Sonneveld, T. T. Rosalina, B. E. Vos, K. A. Jansen, G. W. M. Peters, F. N. Van De Vosse, G. H. Koenderink, *Langmuir* **2017**, *33*, 6342.
- [24] M. Jaspers, S. L. Vaessen, P. van Schayik, D. Voerman, A. E. Rowan, P. H. J. Kouwer, *Nat. Commun.* **2017**, *8*, 15478.
- [25] L. Bidault, M. Deneufchatel, C. Vancaeyzeele, O. Fichet, V. Larreta-Garde, *Biomacromolecules* **2013**, *14*, 3870.
- [26] D. Dikovskiy, H. Bianco-Peled, D. Seliktar, *Biomaterials* **2006**, *27*, 1496.
- [27] J. C. Rose, M. Cámara-Torres, K. Rahimi, J. Köhler, M. Möller, L. De Laporte, *Nano Lett.* **2017**, *17*, 3782.
- [28] K. Y. T. Chan, C. Zhao, E. M. J. Siren, J. C. Y. Chan, J. Boschman, C. J. Kastrup, *Biomacromolecules* **2016**, *17*, 2248.
- [29] J. C. Rose, D. B. Gehlen, T. Haraszti, J. Köhler, C. J. Licht, L. De Laporte, *Biomaterials* **2018**, *163*, 128.
- [30] A. Omidinia-Anarkoli, S. Boesveld, U. Tuvshindorj, J. C. Rose, T. Haraszti, L. De Laporte, *Small* **2017**, *13*, 1702207.
- [31] Y. Zhang, P. Heher, J. Hilborn, H. Redl, D. A. Ossipov, *Acta Biomater.* **2016**, *38*, 23.
- [32] L. W. Chan, X. Wang, H. Wei, L. D. Pozzo, N. J. White, S. H. Pun, *Sci. Transl. Med.* **2015**, *7*, 277ra29.
- [33] Y. Maeda, T. Nakamura, I. Ikeda, *Macromolecules* **2002**, *35*, 217.
- [34] H. Vihola, A. Laukkanen, L. Valtola, H. Tenhu, J. Hirvonen, *Biomaterials* **2005**, *26*, 3055.
- [35] H. Peng, M. Kather, K. Rübsam, F. Jakob, U. Schwaneberg, A. Pich, *Macromolecules* **2015**, *48*, 4256.
- [36] H. Peng, W. Xu, A. Pich, *Polym. Chem.* **2016**, *7*, 5011.
- [37] H. Peng, K. Rübsam, X. Huang, F. Jakob, M. Karperien, U. Schwaneberg, A. Pich, *Macromolecules* **2016**, *49*, 7141.
- [38] H. Peng, K. Rübsam, C. Hu, F. Jakob, U. Schwaneberg, A. Pich, *Biomacromolecules* **2019**, *20*, 992.
- [39] K. Matyjaszewski, J. Xia, *Chem. Rev.* **2001**, *101*, 2921.
- [40] K. Matyjaszewski, N. V. Tsarevsky, *Nat. Chem.* **2009**, *1*, 276.
- [41] J. Nicolas, Y. Guillauneuf, C. Lefay, D. Bertin, D. Gigmes, B. Charleux, *Prog. Polym. Sci.* **2013**, *38*, 63.
- [42] V. Sciannamea, R. Jérôme, C. Detrembleur, *Chem. Rev.* **2008**, *108*, 1104.
- [43] C. Boyer, V. Bulmus, T. P. Davis, V. Ladmiral, J. Liu, S. Perrier, *Chem. Rev.* **2009**, *109*, 5402.
- [44] G. Moad, E. Rizzardo, S. H. Thang, *Aust. J. Chem.* **2005**, *58*, 379.
- [45] G. Moad, E. Rizzardo, S. H. Thang, *Aust. J. Chem.* **2006**, *59*, 669.
- [46] G. Moad, E. Rizzardo, S. H. Thang, *Polymer* **2008**, *49*, 1079.
- [47] G. Moad, E. Rizzardo, S. H. Thang, *Acc. Chem. Res.* **2008**, *41*, 1133.
- [48] G. Moad, E. Rizzardo, S. H. Thang, *Aust. J. Chem.* **2009**, *62*, 1402.
- [49] G. Moad, J. Chiefari, Y. K. (Bill) Chong, J. Krstina, R. T. A. Mayadunne, A. Postma, E. Rizzardo, S. H. Thang, *Polym. Int.* **2000**, *49*, 993.
- [50] E. Gau, D. M. Mate, Z. Zou, A. Oppermann, A. Töpel, F. Jakob, D. Wöll, U. Schwaneberg, A. Pich, *Biomacromolecules* **2017**, *18*, 2789.
- [51] S. Neuss, C. Apel, P. Buttler, B. Denecke, A. Dhanasingh, X. Ding, D. Grafahrend, A. Groger, K. Hemmrich, A. Herr, W. Jahnen-Dechent, S. Mastitskaya, A. Perez-Bouza, S. Rosewick, J. Salber, M. Wöltje, M. Zenke, *Biomaterials* **2008**, *29*, 302.
- [52] M. S. V. Ferreira, R. K. Schneider, W. Wagner, W. Jahnen-Dechent, N. Labude, M. Bovi, D. Piroth, R. Knüchel, T. Hieronymus, A. M. Müller, M. Zenke, S. Neuss, *Tissue Eng., Part C* **2013**, *19*, 25.
- [53] J. Van De Kamp, W. Jahnen-Dechent, B. Rath, R. Knuechel, S. Neuss, *Stem Cells Int.* **2013**, *2013*, 892065.
- [54] M. S. Ventura Ferreira, W. Jahnen-Dechent, N. Labude, M. Bovi, T. Hieronymus, M. Zenke, R. K. Schneider, S. Neuss, *Biomaterials* **2012**, *33*, 6987.
- [55] M. S. Ventura Ferreira, W. Jahnen-Dechent, N. Labude, M. Bovi, T. Hieronymus, M. Zenke, R. K. Schneider, S. Neuss, *Biomaterials* **2012**, *33*, 9165.
- [56] T. M. Lammens, J. Potting, J. P. M. Sanders, I. J. M. De Boer, *Environ. Sci. Technol.* **2011**, *45*, 8521.
- [57] A. L. Harreus, R. Backes, J.-O. Eichler, R. Feuerhake, C. Jäkel, U. Mahn, R. Pinkos, R. Vogelsang, *Ullmann's Encyclopedia of Industrial Chemistry*, Wiley-VCH, Weinheim, Germany **2011**.
- [58] Y. Louven, K. Schute, R. Palkovits, *ChemCatChem* **2019**, *11*, 439.
- [59] M. Beija, J.-D. Marty, M. Destarac, *Chem. Commun.* **2011**, *47*, 2826.
- [60] M. F. Pittenger, *Science* **1999**, *284*, 143.
- [61] S. E. Haynesworth, J. Goshima, V. M. Goldberg, A. I. Caplan, *Bone* **1992**, *13*, 81.
- [62] S. Neuss, R. K. M. Schneider, L. Tietze, R. Knüchel, W. Jahnen-Dechent, *Cells Tissues Organs* **2010**, *191*, 36.